28 Oct 1992

Line Emission From C⁶⁺, O8+ + Li Electron Capture Collisions

Ronald E. Olson
Missouri University of Science and Technology, olson@mst.edu

J. Pascale

R. Hoekstra

Recommended Citation

R. E. Olson et al., "Line Emission From C⁶⁺, O8+ + Li Electron Capture Collisions," *Journal of Physics B: Atomic, Molecular and Optical Physics*, vol. 25, no. 20, pp. 4241 - 4247, IOP Publishing, Oct 1992.
The definitive version is available at https://doi.org/10.1088/0953-4075/25/20/019

Journal of Physics B: Atomic, Molecular and Optical Physics

Line emission from C^{6+}, O^{8+} + Li electron capture collisions

To cite this article: R E Olson *et al* 1992 *J. Phys. B: At. Mol. Opt. Phys.* **25** 4241

J. Phys. B: At. Mol. Opt. Phys. **25** (1992) 4241-4247. Printed in the UK

Line emission from C^{6+}, $O^{8+}+Li$ electron capture collisions

R E Olson†, J Pascale‡ and R Hoekstra§

† Physics Department, University of Missouri-Rolla, Rolla, MO 65401, USA
‡ Service des Photons, Atomes et Molecules, Centre d'Etudes de Saclay, 91191 Gif-sur-Yvette Cedex, France
§ Kernfysisch Versneller Instituut, Zernikelaan 25, 9747 AA Groningen, The Netherlands

Received 19 May 1992

Abstract. Electron capture cross sections to $n\ell$ sublevels have been calculated for 1-10 keV u^{-1} collisions of C^{6+} and O^{8+} projectiles on a Li target. The classical trajectory Monte Carlo method has been employed with the initial phase distributions for the Li(2s) target obtained from Hartree-Fock calculations. The cross sections are found to maximize at $n=7$ for C^{6+} and $n=8$-9 for O^{8+}. The $n\ell$ cross sections were used to calculate $\Delta n=1$ line emission cross sections. Comparison of these cross sections with the experimental results of Wolfrum *et al* indicates good agreement between theory and experiment.

1. Introduction

Electron capture collisions between C^{q+} and O^{q+} ions and Li atoms are of considerable practical interest. The $n\ell$ sublevel cross sections are needed to obtain line emission cross sections for plasma diagnostics in current and future tokamak nuclear fusion reactors. Present and planned plasma diagnostics for modelling ion transport monitor line emission from electron capture reactions employing injected Li pellets and beams. Both C^{q+} and O^{q+} are dominant impurities in tokamak plasmas. The reason for the use of Li atom probes is that the corresponding line emission is removed from the plasma's background radiation, and that the emission cross sections for visible radiation are quite large, especially when compared to diagnostics employing injected H^0 or He^0 beams. Observation of visible radiation is a requirement because of the need to employ remote sensing with the use of fibre optics in a high neutron flux reactor. Li probes are especially sensitive to the important edge, or 'scrape-off' layer of the plasma where the understanding of ion transport is critical to diverter design.

In this paper, we present calculated line emission cross sections for 1 to 10 keV u^{-1} collisions of

$$X^{q+}+\mathrm{Li(2s)}\rightarrow X^{(q-1)+}(n\ell)+\mathrm{Li}^{+} \qquad (1)$$

where X^{q+} is C^{6+} or O^{8+}. The inputs for the line emission cross sections are the partial cross sections to specific principal and orbital angular momentum quantum levels. Comparison is made to the recently published experimental work of Wolfrum *et al* (1992).

In the paper by Wolfrum *et al*, experimental observations of line emission cross sections were compared to predictions based on the classical over-the-barrier model of Ryufuku *et al* (1980) and Niehaus (1986). In general, the agreement was poor, which may be a reflection on either the over-the-barrier model, or the assumptions

0953-4075/92/204241+07$07.50

made about the distributions of the product $n\ell$ sublevels. Calculations based on quantum mechanical models such as atomic- or molecular-orbital expansion techniques are unavailable for the systems under study; the reason being that the size of the basis sets becomes prohibitively large. For the work presented here, it was necessary to include levels up to $n=15$ in order to obtain converged line emission cross sections.

The classical trajectory Monte Carlo (CTMC) method provides an exact classical calculation of the electron capture cross sections. Because of this, a comparison to classical over-the-barrier estimates of the cross sections should be useful. *A priori*, one could argue that the CTMC method should successfully model these collisions, in that the electron capture proceeds to large n principal quantum numbers that are well described classically. Such arguments have been verified for collisions of ions with highly-excited target atoms by Pascale *et al* (1990). Moreover, we employ $n\ell$ sublevel determinations that are based on phase space arguments to the corresponding quantum mechanical quantities. Likewise, the Li(2s) atom target is simulated by using a model potential that is obtained from Hartree–Fock calculations.

Recent work by Meng *et al* (1990) indicates that the n and $n\ell$ cross sections can be accurately predicted for the difficult He and H_2 target systems when the electronic representation of the target is based on model potentials determined from quantum mechanical methods. Moreover, direct comparisons to $He^{2+}+H$ experimental results (Frieling *et al* 1992), indicate good agreement with the CTMC $n\ell$ cross sections (Schultz *et al* 1991). Likewise, CTMC results for C^{6+}, $O^{8+}+H$ ($n=1,2,3$) collisions provided the basis for the analysis of ion transport on the ASDEX tokamak in Garching (Isler and Olson 1988, Olson and Schultz 1989).

2. Theory

The three-dimensional, three-body CTMC method employed here has been thoroughly described in the past (Abrines and Percival 1966, Olson and Salop 1977). For application to a Li-atom target system, the Li(2s) electron is assumed to move in a model potential obtained from Hartree–Fock calculations by Garvey *et al* (1975). The functional form for this model potential is given by

$$V(r)=-[Z-NS(r)]/r \tag{2}$$

with the screening due to the core electrons given by

$$S(r)=1-\{(\eta/\xi)[\exp(\xi r)-1]+1\}^{-1}. \tag{3}$$

In equations (2) and (3), Z and N denote the nuclear charge and number of non-active electrons in the target core, and η and ξ are screening parameters tabulated by Garvey *et al* (1975). The initialization of the target electron was performed by an iterative procedure developed by Reinhold and Falcón (1986).

After the completion of each trajectory, the system is tested for the electron capture reaction. If positive, a classical number n_c is defined which is related to the calculated binding energy E_p of the electron relative to the ionic projectile via

$$E_p=-Z_p^2/(2n_c^2) \tag{4}$$

where Z_p is the charge of the projectile. The value of n_c is then related to the principal quantum number n by the condition (Olson 1981)

$$[(n-\tfrac{1}{2})(n-1)n]^{1/3}\leqslant n_c<[n(n+\tfrac{1}{2})(n+1)]^{1/3}. \tag{5}$$

The orbital angular momentum is determined from the normalized classical angular momentum $\ell_c=(n/n_c)(\boldsymbol{r}\times\boldsymbol{p})$, where $\boldsymbol{r}$ and $\boldsymbol{p}$ are the position vectors of the electron relative to the projectile core. The classical ℓ_c is related to the orbital quantum number ℓ of the final state via

$$\ell\leqslant\ell_c<\ell+1. \tag{6}$$

For the systems under study here, a minimum of 10^5 trajectories were run at each energy in order to insure meaningful results for the emission cross sections. There is a necessity to run a large number of trajectories since the final quantum states extend to large n values with their resulting ℓ values, and cascade corrections to the emission cross sections are significant.

3. Results

The calculated n cross sections for the C^{6+} and $O^{8+}+Li$ systems, each at three separate energies, are presented in figures 1 and 2. As can be readily seen, electron capture proceeds to large principal quantum numbers, with the cross sections maximizing at $n=7$ for the C^{6+} projectile and $n=8$–9 for O^{8+}. The dominant n value has been discussed previously (Olson 1981), and is given approximately by

$$n_{\max}=q^{3/4}/(2E_i)^{1/2} \tag{7}$$

where q is the charge state of the projectile and E_i is the binding energy in atomic units of the target electron. Equation (7) yields $n_{\max}=1.6q^{3/4}$, while inspection of figures 1 and 2 indicates that the constant 1.6 should be 12% larger at about 1.8. Equation (7) is also applicable to capture from excited states (Olson 1980), but is generally valid only at low relative collision velocities, $v\leqslant v_e$, where v_e is the orbital velocity of the target electron.

The exact classical calculation of the cross sections can be compared to the results obtained from the classical over-the-barrier model. This latter model yields a total

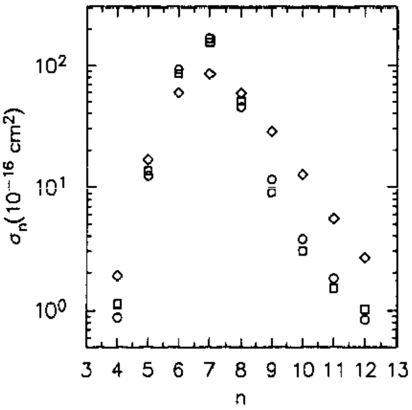

Figure 1. $C^{6+}+Li$ electron capture cross sections to n principal quantum numbers. Collisions at 2.77, 5.08 and 10.0 keV u^{-1} are denoted by circles, squares, and diamonds, respectively.

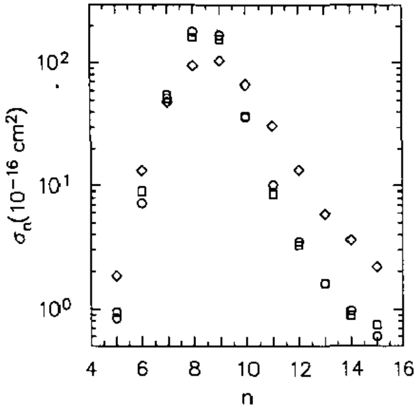

Figure 2. $O^{8+}+Li$ electron capture cross sections to n principal quantum numbers. Collisions at 2.68, 5.08 and 10.0 keV u^{-1} are denoted by circles, squares and diamonds respectively.

electron capture cross section for 4.0 keV u^{-1} C^{6+} of 7.2×10^{-14} cm^2, and partial cross sections for capture to $n=7$ of 4.6×10^{-14} cm^2 and $n=8$ of 2.7×10^{-14} cm^2 (Wolfrum *et al* 1992). The exact results are 3.3×10^{-14}, 1.6×10^{-14} and 4.9×10^{-15} cm^2, respectively. A similar overestimate of the cross sections is obtained for the 4.0 keV u^{-1} O^{8+} system, with total and $n=9$ values given by the over-the-barrier model of 9.5×10^{-14} and 4.9×10^{-14}, while the numerical results are 4.5×10^{-14} and 1.6×10^{-14} cm^2, respectively. This apparent lack of agreement may rest in the difficulty of partitioning the product cross section to specific n values within the over-the-barrier model.

The n-value cross sections are relatively energy independent, as seen in figures 1 and 2. Only at the highest energy, 10 keV u^{-1}, do we observe the expected broadening of the n distributions. The n distributions are narrowly peaked, and deviate strongly from a $1/n^3$ scaling expected from phase space arguments. One should also note that the partial cross sections are quite significant, even at n values as large as $n=15$.

It is difficult to present all the $n\ell$ cross sections computed for this study. Results for 5.08 keV u^{-1} collisions are given in tables 1 and 2. As has been noted previously for collisions involving H(1s) targets (Olson 1981), the large angular momentum states are preferentially populated for principal quantum numbers n less than n_{max}, while at n values greater than n_{max} the ℓ distributions are very non-statistical and in fact

Table 1. $n\ell$ cross sections (units 10^{-16} cm^2) for 5.08 keV u^{-1} $C^{6+}+Li$ collisions. The statistical error of these cross sections (two standard deviations) may be evaluated from $\Delta\sigma_{n\ell}(10^{-16}\ cm^2)=0.113\sigma_{n\ell}^{1/2}$.

	l								
n	0	1	2	3	4	5	6	7	8
5	0.2	1.3	2.6	4.0	5.2				
6	0.2	2.0	6.8	17.5	26.2	33.1			
7	0.2	1.2	3.2	9.4	22.9	46.3	71.1		
8	0.1	0.6	1.3	2.8	5.9	10.5	13.7	16.4	
9	0.1	0.4	0.6	0.9	1.3	1.8	1.8	1.1	1.0

Table 2. $n\ell$ cross sections (units $10^{-16}\,\mathrm{cm}^2$) for 5.08 keV u^{-1} O^{8+} + Li collisions. The statistical error of these cross sections (two standard deviations) may be evaluated from $\Delta\sigma_{n\ell}(10^{-16}\,\mathrm{cm}^2) = 0.131\sigma_{n\ell}^{1/2}$.

	l										
n	0	1	2	3	4	5	6	7	8	9	10
6	0.1	0.6	1.3	1.8	2.5	2.8					
7	0.1	1.1	3.9	8.6	12.1	14.4	15.3				
8	0.1	0.8	2.7	9.1	21.7	35.7	45.3	46.5			
9	0.0	0.5	1.2	3.0	8.1	17.9	31.8	43.3	50.1		
10	0.0	0.3	0.6	1.2	2.1	4.3	6.5	7.6	7.0	7.8	
11	0.0	0.2	0.3	0.5	0.8	1.1	1.6	1.6	1.2	0.7	0.6

display a maximum at intermediate ℓ values. The maximum is closely related to the magnitude of $\boldsymbol{\ell} = \boldsymbol{b} \times \boldsymbol{v}$, where $\boldsymbol{b}$ corresponds to the impact parameter range which has a maximum contribution to the total cross section, and $\boldsymbol{v}$ is the velocity of the electron that was transferred to the projectile centre. From the calculated transition probabilities, we find a maximum contribution to the total cross section at $b = 15\,a_0$ for C^{6+} and $b = 17\,a_0$ for O^{8+}. For a projectile velocity corresponding to 5.08 keV u^{-1}, the above impact parameters yield angular momentum magnitudes of 6.8 and 7.7 for C^{6+} and O^{8+}, respectively. For the $n = 9$ calculations with C^{6+}, and $n = 11$ results for O^{8+}, tables 1 and 2, the predicted maxima are very close to the numerical results. Calculations for the higher n values show these trends continue, however, the numerical statistics are poor.

A major reason for this study is to test the results of CTMC calculations against the recently published line emission cross sections of Wolfrum *et al* (1992). If the comparisons between theory and experiment are reasonable, added confidence is given to the theory being able to make predictions of the line emission cross sections needed for high temperature plasma diagnostics. In particular, we have concentrated on $\Delta n = 1$ transitions in the visible region, which are the most useful for remote sensing on tokamak nuclear fusion reactors employing fibre optics.

The C^{6+} + Li line emission cross sections are given in figure 3. For the 7 → 6 and the 8 → 7 transitions, the experimental data of Wolfrum *et al* are available for comparison. For the 7 → 6 transition, theory and experiment agree to within 10%, except at energies below 2.5 keV u^{-1} where theory overestimates the data by up to 32% at 1.85 keV u^{-1}. The comparison for the 8 → 7 transition is also favourable, with theory tending to underestimate the data at intermediate energies by approximately 25%. Again the energy dependences of the theoretical values do not decrease as rapidly as the experiment at the lowest energies. The experimental data have statistical errors as shown in the figure, plus absolute uncertainties of approximately 20%-25%. Thus, it appears the CTMC calculation of the partial cross sections, and in particular those for the largest ℓ values within a given n value, are well represented. It is these latter large ℓ values that make a dominant contribution to the emission cross sections because of their transition strengths.

The line emission cross sections for the O^{8+} + Li system are displayed in figure 4. Unfortunately, there are no experimental data to directly compare to the calculated results. However, data for the similar Ne^{8+} + Li system have been measured by Wolfrum *et al* (1992) for the 9 → 8 transition at 434.2 nm. The calculated cross section for the

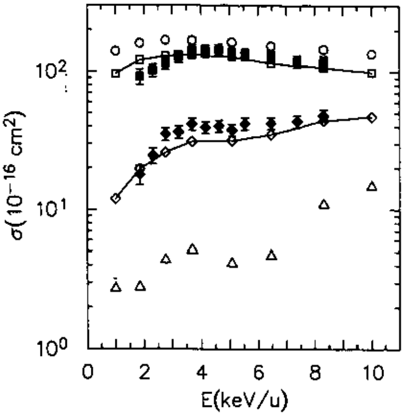

Figure 3. Calculated line emission cross sections for C^{6+} + Li electron capture collisions are given by the open circles, squares, diamonds and triangles for the 6→5 (207.1 nm), 7→6 (343.5 nm), 8→7 (529.2 nm) and 9→8 (771.9 nm) transitions, respectively. The experimental data of Wolfrum *et al* (1992) for the 7→6 and 8→7 transitions are given by the full squares and diamonds, respectively. A line has been placed through the corresponding calculated values to aid the eye in the comparison between theory and experiment.

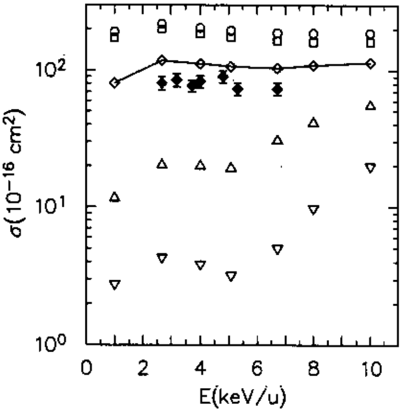

Figure 4. Calculated line emission cross sections for O^{8+} + Li electron capture collisions are given by the open circles, squares, diamonds, triangles and inverted triangles for the 7→6 (193.2 nm), 8→7 (297.7 nm), and 9→8 (434.2 nm), 10→9 (607.0 nm) and 11→10 (820.4 nm) transitions, respectively. The experimental data of Wolfrum *et al* (1992) for the 9→8 transition with a Ne^{8+} projectile are given by the full diamonds. A line has been placed through the corresponding calculated values to aid the eye in the comparson between theory (O^{8+}) and experiment (Ne^{8+}).

same transition in the O^{8+} system tend to lie approximately 40% above the experimental results which have an absolute uncertainty of only 20%.

We do not expect that the K-shell electrons on the Ne^{8+} projectile will greatly effect the comparison to O^{8+}. The reasons for this assumption is that the cross sections are determined at large impact parameters where the asymptotic charge is 8+. Moreover, the *n*s and *n*p levels that have large quantum defects and interact strongly with the core, contribute a negligible amount to the emission cross sections. These conclusions are consistent with the detailed studies of Harel and Jouin (1988) and Harel and Salin

(1988) for similar projectiles colliding with H(1s), that is at these energies the Ne^{8+} should yield cross section results very similar to O^{8+}. However, only a direct measurement on the O^{8+} + Li system can test the above assumptions. The emission cross sections for the $10\rightarrow 9$ and $11\rightarrow 10$ transitions are found to display rapidly increasing values for energies above 6 keV u^{-1}. This is due to the broadening of the n distribution, figure 2, with increasing velocity.

In conclusion, electron capture to high-lying quantum levels is reasonably predicted for multiply-charged C^{6+} and O^{8+} projectile impact on Li. Where a direct comparison can be made between theory and experiment, C^{6+}, there is good agreement. For the O^{8+} system, discrepancies on the order of 40% are observed when comparison is made to the Ne^{8+} system. The exact numerical classical calculations presented here display major differences with the predictions of the classical over-the-barrier model in both the overall total cross section and in the partial cross sections to specific n levels.

Acknowledgments

The authors would like to thank Dr Ralph Isler for providing the computer code used to obtain line emission cross sections from the calculated $n\ell$ cross sections. This work was supported by the US Department of Energy, Office of Fusion Energy.

References

Abrines R and Percival I C 1966 *Proc. Phys. Soc.* **88** 861

Garvey R H, Jackman C H and Green A E S 1975 *Phys. Rev.* A **12** 1144

Frieling G J, Hoekstra R, Smulders E, Dickson W, Zinoviev A N, Kuppens S J and de Heer F J 1992 *J. Phys. B: At. Mol. Opt. Phys.* **25** 1245

Harel C and Jouin H 1988 *J. Phys. B: At. Mol. Opt. Phys.* **21** 1988

Harel C and Salin A 1988 *Electronic and Atomic Collisions* ed H B Gilbody, W R Newell, F H Read and A C H Smith (Amsterdam: Elsevier) pp 631–42

Isler R C and Olson R E 1988 *Phys. Rev.* A **37** 3399

Meng L, Reinhold C O and Olson R E 1990 *Phys. Rev.* A **42** 5286

Niehaus A 1986 *J. Phys. B: At. Mol. Phys.* **19** 2925

Olson R E 1980 *J. Phys. B: At. Mol. Phys.* **13** 483

—— *1981 Phys. Rev.* A **24** *1726*

Olson R E and Salop A 1977 *Phys. Rev.* A **16** 531

Olson R E and Schultz D R 1989 *Phys. Scr.* T **28** 71

Pascale J, Olson R E and Reinhold C O 1990 *Phys. Rev.* A **42** 5305

Reinhold C O and Falcón C A 1986 *Phys. Rev.* A **33** 3859

Ryufuku H, Sasaki K and Watanabe T 1980 *Phys. Rev.* A **21** 745

Schultz D R, Meng L, Reinhold C O and Olson R E 1991 *Phys. Scr.* T **37** 89

Wolfrum E, Hoekstra R, de Heer F J, Morgenstern R and Winter H 1992 *J. Phys. B: At. Mol. Opt. Phys.* **25** 2597